Sigma Journal of Engineering and Natural Sciences
Web page info: https://sigma.yildiz.edu.tr
DOI: 10.14744/sigma.2026.1966

Research Article

Commiphora myrrha-functionalized bacterial cellulose as a potential wound healing biomaterial

Seda GENÇ ŞİMŞEK[1], Cenk DENKTAŞ[2,*], Nelisa TÜRKOĞLU[1]

[1]*Department of Molecular Biology and Genetics, Yildiz Technical University, 34220, İstanbul, Türkiye*
[2]*Department of Physics, Yildiz Technical University, İstanbul, 34220, Türkiye*

ARTICLE INFO

Article history
Received: 07 June 2024
Revised: 21 August 2024
Accepted: 03 October 2024

Keywords:
Bacterial Cellulose; Commiphora Myrrha; Wound Healing

ABSTRACT

Bacterial cellulose (BC) is a valuable biomaterial for wound treatment due to its strong biocompatibility, porous structure, and mechanical strength. This study prepared BC membranes enriched with *myrrh* to enable them to contribute more effectively and rapidly to the wound healing process. *Commiphora myrrha*, a traditional medicinal plant known for its healing properties, was incorporated into the BC structure for the first time in this study; its physicochemical properties and cellular behavior were examined. Scanning electron microscopy (SEM) and atomic force microscopy (AFM) analyses conducted to examine morphological properties demonstrated that *myrrh* resin was successfully incorporated into the nanofiber network of BC. Fourier-transform infrared spectroscopy (FTIR), thermogravimetric analysis (TGA), and X-ray diffraction (XRD) analyses showed that increased *myrrh* content in BC films led to stronger intermolecular interactions within the membrane, which in turn supported enhanced thermal stability. According to the MTT test results performed using L929 mouse fibroblast cells, all biopolymers showed over 80% cell viability and were found to have no cytotoxic effect. Furthermore, it was noted that BC/mure composite films significantly increased cell adhesion and proliferation. Specifically, a 146.92% increase in cell adhesion was observed up to the 7th day in the BC membrane containing 2.5% mure. These findings indicate that the addition of mure improves the hydrogen bonding capacity, thermal properties, and cell compatibility of BC. The resulting natural composite structure can be considered a strong candidate for use in wound healing by supporting three-dimensional extracellular matrix formation and tissue regeneration.

Cite this article as: Genç Şimşek S, Denktaş C, Türkoğlu N. *Commiphora myrrha*-functionalızed bacterial cellulose as a potential wound healing biomaterial. Sigma J Eng Nat Sci 2026;44(1):42–54.

INTODUCTION

The skin is the body's largest organ, covering its entirety and serving as both a physical and chemical barrier against pathogens, external substances, and dehydration [1]. Additionally, the skin fulfills many important functions such as protecting internal organs, providing sensory sensation, self-repair, and maintaining selective permeability

***Corresponding author.**
*E-mail address: cdenktas@yildiz.edu.tr

This paper was recommended for publication in revised form by Editor-in-Chief Ahmet Selim Dalkilic

[2]. The skin is structurally composed of three main layers: the epidermis, the dermis, and the hypodermis [3]: Wounds are generally classified according to the skin layers involved and the extent of the affected area. "Superficial wounds" involve only the outermost layer, the epidermis. "Partial-thickness wounds" affect both the epidermis and deeper dermal layers and may potentially involve blood vessels, sweat glands, and hair follicles. "Full-thickness wounds," on the other hand, result from injuries that extend from the epidermis and dermis to the subcutaneous fat tissue or deeper tissues [4,5].

A wound is any disruption in the skin's natural state caused by various medical factors, including mechanical, thermal, electrical, chemical, or physiological disturbances [6]. Wounds are generally categorized as either acute or chronic based on their healing process [7]. The primary goal of wound management is to facilitate rapid healing to prevent infection and reduce pain, discomfort, and scarring. Consequently, significant research has focused on developing wound dressings that support the healing process. These dressings can be produced in several forms, such as films, hydrocolloids, hydrogels, microneedles, and foams, using natural biomaterials like chitin, alginate, polyvinyl alcohol, cellulose, hyaluronic acid, starch, collagen, and gelatin [1,8].

An effective wound dressing should ideally [9]: i) enable quick and cost-effective healing, ii) create a suitable environment for epidermal regeneration, iii) offer mechanical support, iv) be biocompatible, v) maintain a moist environment conducive to healing, vi) possess anti-inflammatory and antimicrobial properties, and vii) be easy to manufacture and store. Wound healing is a complex biological process that involves a range of interactions between different cells and matrix components to restore the integrity of damaged tissue. This process unfolds through a series of stages that require the coordinated interplay of various biological systems to fully cover the wound [8]. The wound healing process involves a series of phases that collaborate to rebuild tissue integrity. It begins with hemostasis, where bleeding is stopped through clot formation [10]. This is followed by the inflammatory phase, which serves to protect against infection by employing immune cells to remove pathogens [11]. The next phase is proliferation, during which tissue repair and regeneration occur, marked by the formation of a new extracellular matrix and collagen synthesis [12]. Finally, the maturation and remodeling phase strengthens the newly formed tissue and matures the scar tissue, gradually returning the wound to a state similar to uninjured skin [13]. Each phase is crucial to achieving successful and complete healing.

Traditional wound dressings do not retain the necessary moisture at an adequate level and cannot fully support the healing process. Therefore, biomaterials such as BC have been proposed as a better alternative for use in tissue engineering. BC is a natural polymer formed by the linkage of glucose monomers via β(1→4) glycosidic bonds [14]. Its physicochemical and biological properties make it highly advantageous for wound dressing applications. BC, produced by non-pathogenic bacteria such as Gluconacetobacter xylinum, is notable for its high purity, durability, and lack of components found in plant cellulose, such as lignin, hemicellulose, and pectin [15,16]. This helps it provide a stronger, more porous, and purer structure.

BC's non-toxicity, moisture retention properties, lack of allergenicity, pain-reducing properties, and ease of removal without damaging tissues make it ideal for wound care. Studies in the literature have shown BC to be effective in burns [17], diabetic wounds [18], acute wounds [19], and infected wounds [20]. BC's three-dimensional nanofiber network supports cell adhesion, migration, and proliferation; it facilitates gas exchange by enabling the slow release of drugs. Its high water retention capacity helps control wound exudate, while its flexible structure allows for easy use even on irregular surfaces [21]. Furthermore, its semi-transparent appearance allows for better observation of the wound healing process [15]. BC can be combined with different biological agents or polymers to provide additional benefits to wound healing properties. In this study, *Commiphora myrrha* extract was added to the BC structure to increase fibroblast cell proliferation.

There is no study in the literature on the combined use of BC and *myrrh* resin. This resin, obtained from Commiphora species, has been used in wound care for many years due to its antimicrobial, antioxidant, and anti-inflammatory effects [22]. Adding this natural, economical, and biodegradable resin, known for its properties such as promoting wound dryness and supporting cleanliness, to BC is an approach that could enhance wound healing.

Although bacterial cellulose has been frequently studied in wound care, the combination of BC with *Commiphora myrrha* has not been previously addressed. The novelty of this study is that *myrrh*-enhanced BC membranes increase biocompatibility and promote fibroblast cell growth. This new approach offers an economical, sustainable, and biodegradable solution that can meet the biological requirements for wound healing. We believe our study will contribute to the literature on composite biomaterials and offer the healthcare sector a new alternative, particularly for the treatment of chronic and difficult-to-heal wounds.

MATERIAL AND METHOD

Materials

Gluconacetobacter xylinus (ATCC® 10245TM) was purchased from Formslab. *Commiphora myrrha* was obtained from Yaren Herbalist (Türkiye), a producer of organic and herbal products. All materials used in the bacterial cellulose synthesis were purchased from Sigma-Aldrich, USA. Peptone was of biotechnological grade, yeast extract was of molecular biology grade, glucose had a purity of 99.5% (GC), potassium phosphate monobasic (KH_2PO_4) was

an ACS reagent with 99.0% purity, and potassium phosphate dibasic K_2HPO_4 had a purity of 98%. For cell culture DMEM (high glucose, with glutamine), F-12 Nutrient Mixture (Ham's), Fetal Bovine Serum, and Trypsin EDTA (0.05%) procured from Capricorn Scientific (Germany) were utilized.

Production and Purification of Bacterial Cellulose

Bacterial cellulose (BC) membranes were synthesized using *Acetobacter xylinum* (ATCC® 10245TM). The bacteria were cultured in a static environment using Hestrin and Schramm (HS) liquid medium. The medium composition included 20 g/L glucose, 10 g/L bactopeptone, 10 g/L yeast extract, 4 mM KH_2PO_4, and 6 mM K_2HPO_4, with the pH adjusted to 5.0 by adding 1M HCl. Before use, the medium was sterilized at 120°C for 15 minutes. For inoculation, *A. xylinum* was pre-cultured for 2 days at 30°C using a rotary shaker. BC production occurred by transferring the inoculum to Petri dishes at a 1:10 ratio, where the culture was left undisturbed. Over a 7-day incubation period, BC nanofibers developed in a bacteriological incubator. Following incubation, the membranes were harvested and treated with 1% (w/v) NaOH at 80°C for 2 hours to remove residual bacteria [23]. Finally, the membranes were washed with distilled water to reach a pH of 7.0, then lyophilized and dried.

Preparation Of Bc/*Myrrh* Membranes

The powdered *myrrh* was dissolved in distilled water (1.5%, 2.5%, 5% by mass) at 400 rpm using a magnetic stirrer at 90°C for 4 h. The *myrrh* extract solution was then centrifuged at 10,000 rpm for 10 min and the supernatant was transferred to clean vials. Dried pure BC membranes were immersed in liquid *myrrh* extract solutions prepared at different ratios. Membranes were kept at room temperature for 24 hours. The next day the membranes were removed from the solutions and stored at +4 °C for analysis. Pure BC and BC membranes containing 1.5%, 2.5%, and 5% *myrrh* extract by mass were designated BC/M0, BC/M1, BC/M2, and BC/M3, respectively.

Characterization

Morphology of BC and BC/*Myrrh* membranes

The morphological properties of pure BC and composite BC/*Myrrh* membranes were determined by scanning electron microscope (SEM) (Zeiss Evo LS10) and atomic force microscope (AFM) (Shimadzu SPM 9600, Japan). For the analyses, the membranes were dried and then used. Before SEM analysis Au-Pd coating (Quorum SC-7620) was performed on samples for 1 min. The samples were examined at 20.00 KX magnification for SEM analysis and 2.5 nm magnification for AFM analysis.

Micro-structure of BC and BC/*Myrrh* membranes

The molecular structure and identification of intramolecular functional groups in all samples were examined using Fourier transform infrared (FTIR) spectroscopy (Perkin Elmer Inc., USA). The analysis was conducted over a wavenumber range of 4000–500 cm^{-1}. The spectra were collected with 32 scans at a resolution of 4 cm^{-1}.

Thermal analysis

The thermal stability of the produced membranes was assessed through thermogravimetric (TG) analysis using the SII6000 Exstar TG 6300. The average dry weight of the samples was around 1 mg, and all analyses were conducted under an inert nitrogen (N_2) atmosphere. A heating rate of 10 °C/min was used, with mass loss measured over 90 minutes, spanning a temperature range of 30 °C to 700 °C. The thermograms for each sample were then evaluated.

X-ray diffraction (XRD)

Crystallinity and amorphous of bacterial celluloses were determined using an X-ray diffractometer. The X-ray generator tension and current were 45 kV and 40 mA, respectively.

The swellıng analysıs of BC and BC/*Myrrh* membranes

The water retention degree of the membranes was determined by the swelling test [24]. Membranes (triplicates) were cut into 1 cm^2 square shapes and their dry weight was measured (W_0). Then, it was immersed in distilled water at room temperature (25 °C) for 24 h. The weights of the swollen membranes (W_s) were measured at regular intervals. The water retention rate of the samples was calculated using the following equation;

$$Swelling\ ratio = (W_S - W_{0)}/W_0 \quad (1)$$

W_0 represents the weight of the dry membrane and W_s represents the weight of the swollen membrane. The weight of the swollen membranes was measured after removing excess water from the surface using filter paper.

***In Vitro* Cytotoxicity Studies**

Cell viability

The in vitro cytotoxicity of the membranes on L929 mouse fibroblast cells (ATCC® CRL-6364™) was evaluated using the MTT assay [25]. The L929 cells were cultured in DMEM F-12 medium supplemented with 10% FBS and seeded in a 96-well plate at a density of 10^5 cells per well. The plate was incubated at 37 °C with 5% CO_2 for 24 hours. Following this incubation, the medium was removed, and the membranes, sterilized under UV light for 1 hour and cut into disk shapes, were placed in the wells with fresh medium. After another 24-hour incubation, the medium was replaced with 100 µL of MTT solution (5 mg/mL in medium), and the cells were incubated for 4 hours. The MTT solution was then removed, and 100 µL of dimethyl sulfoxide (DMSO) was added to dissolve the formazan crystals. The optical density was measured at 570 nm using an ELISA reader (Thermo Scientific Multiskan Go, USA).

Cell adhesion

Cell proliferation and adhesion properties on membranes were determined using the MTT assay [26]. In the study, L929 fibroblast cells cultured in DMEM F-12 medium supplemented with 10% FBS and 1% L-glutamine and maintained at 37°C in a 5% CO_2 environment were used. Membranes were cut into 1 cm x 1 cm pieces and placed in 24-well plates. 10^3 fibroblast cells were seeded onto each membrane and incubated for 24 hours. Cell adhesion and proliferation were tested on days 1, 3, and 7. After each time period, the membranes were placed in new 24-well plates, and 400 µL of MTT solution (5 mg/mL in the medium) was added to each well. After a 4-hour incubation, the medium was removed, and 400 µL of DMSO was added to dissolve the formazan crystals. Finally, cell viability was measured at an absorbance value of 570 nm.

Statıstical Analysis

Statistical comparisons were performed using *t*-test analysis. p values < 0.05 were considered statistically significant.

RESULTS AND DISCUSSION

Morphology of BC and BC/*Myrrh* Membranes

The surface morphological and topological properties of freeze-dried pure BC and BC/*Myrrh* membranes were determined by SEM and AFM analysis. The images of all membranes examined by SEM are shown in Figure 1. Pure BC is characterized by a three-dimensional (3D) nanofiber network structure. Thus, the BC matrix has a randomly arranged porous geometric structure [27]. BC makes it possible to impregnate various materials with different physical properties due to its unique morphology [28]. Pure BC membranes (Fig. 1a) exhibited a 3D network structure composed of interconnected fibrils. We found that the pure BC membrane morphology is compatible with the BC structure described in the literature.

Some changes in cellulose structure compared to pure BC were found when the *myrrh*-doped BC membrane was examined (Fig. 1b-d). The material surface is more irregular and complex. A thicker fiber network structure with the effect of *myrrh* and *myrrh*-induced spherical agglomerates appeared.

The formation of a flat surface due to the layer created by *myrrh* extract coating the BC is seen in Figure.1c. and the highest *myrrh* extract concentration leads to a thicker flat surface in Fig. 1d. Briefly, we can conclude depending on the increasing *myrrh* concentration, the porosity decreases in BC membranes, and a smooth layer is formed in BC/*Myrrh* membranes. Nevertheless, the 3D nanofiber network structure can still be observed in *myrrh*-doped membranes. According to the morphological findings

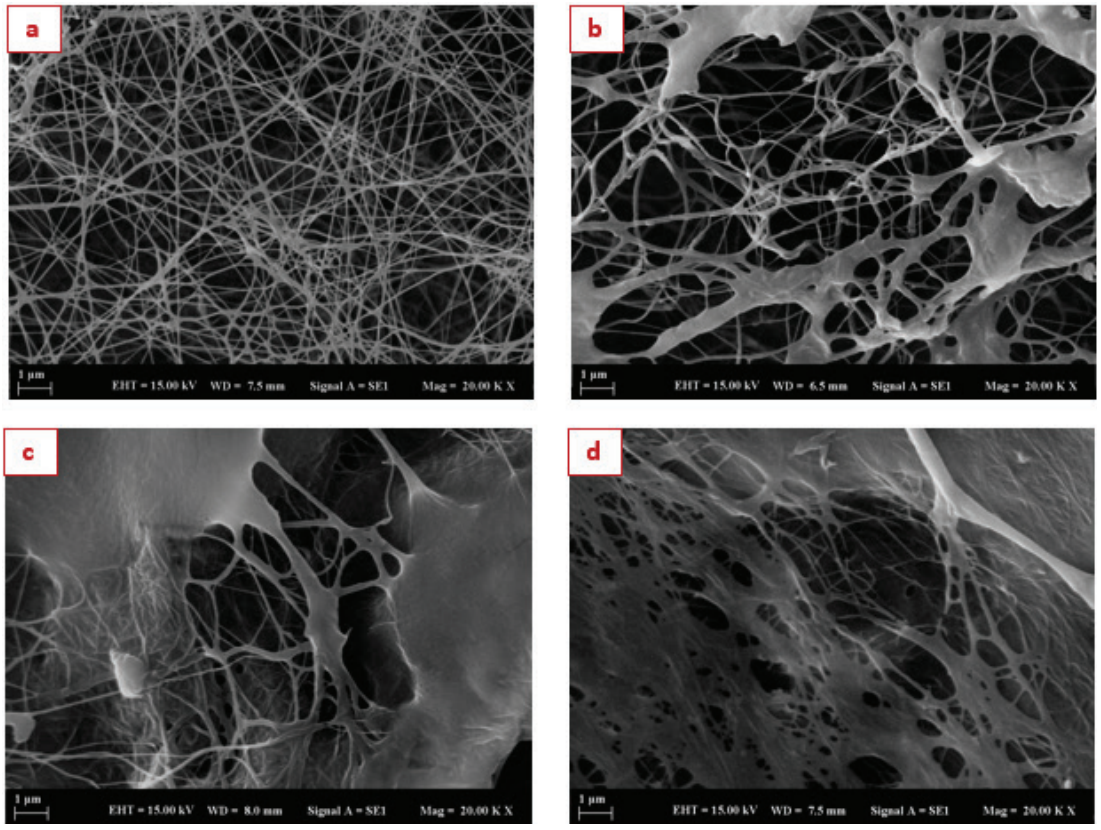

Figure 1. SEM images of all membranes: (a) BC/M0, (b) BC/M1, (c) BC/M2, (d) BC/M3 at 20.00 KX magnification.

of *myrrh*-doped BC membranes, a compact structure is observed in which *myrrh* can penetrate the BC surface and interact with microfibrils.

AFM images were obtained to visualize the surface topography of BC and BC/*Myrrh* membranes (Fig. 2). While pure BC membranes showed a clear nanofiber network structure, *myrrh*-added BC membranes exhibited unclear fibrous network structure. The findings obtained from AFM and SEM analyses confirm each other. Both analyses confirm that *myrrh*, a bioactive molecule, can be incorporated into BC membranes. When the morphologies of BC and BC/*Myrrh* membranes are examined, it is reported that interconnected fibers provide the necessary structure for cell adhesion and proliferation for tissue engineering applications [29]. Our results are consistent with the morphological characterization of the membranes obtained with pure BC and plant extract [30], vaccarin [26], lignin [31], and chitosan [32] doped BC composite materials in the literature.

ATR/FTIR Analysis of Membranes

The ATR/FTIR spectra of pure BC and *myrrh* extract doped celluloses are shown in Figure 3. The differences between the FTIR results of pure BC and BC/*Myrrh* composites indicate that there may be strong interactions between cellulose and *myrrh* molecules (see Fig.3). It is seen from Figure 3. that the peak at 3343 cm^{-1} in pure BC corresponds to the O-H stretching vibration in cellulose I and the peak at 3243 cm^{-1} corresponds to hydrogen-bound O-H [33,34]. As the *myrrh* extract content in BC increased, the OH-strain peak shifted to a higher wavenumber (from 3248 cm^{-1} to 3273 cm^{-1}). This result indicates that the OH groups in the *myrrh* molecule enhance the hydrogen bonding effect in the structure of the composites [35]. The range 3000-2750 cm^{-1} is also attributed to C-H stretching peaks. The intensity of the 1633 cm^{-1} peak [36], which is due to the H-O-H bending vibration of bound water molecules in cellulose, was found to change as a result of *myrrh* addition. In pure BC, a peak (1428 cm^{-1}) corresponding to CH_2 bending associated with the crystalline/amorphous ratio in some cellulose molecules was detected [37]. The interaction with *myrrh* resulted in a significant change in the peak intensity of the CH_2 bending. This change is an indication that it corresponds to a higher degree of crystallinity [37,38]. Although the peaks at 1161, 1108, 1056, and 1031 cm^{-1} in pure BC were evaluated by different authors [39-41] these peaks can be assigned to C-C stretching vibration, skeletal vibration, and ring vibration, respectively [42,43]. The peak at 898 cm^{-1} corresponding to crystallized cellulose-I in pure BC [36] was shifted to a higher wave number (926 cm^{-1}) upon interaction with *myrrh.* This result is evidence of the change in the crystal structure due to the presence of *myrrh* extract in BC. A new peak was also detected at 848 cm^{-1}. This peak is associated with *Commiphora* resin, commonly known as *myrrh*, one of the three major genera of the Burseraceae family [44,45]. As a result of the interaction between pure BC and *myrrh* extract, the peak at 663 cm^{-1} in pure BC disappeared.

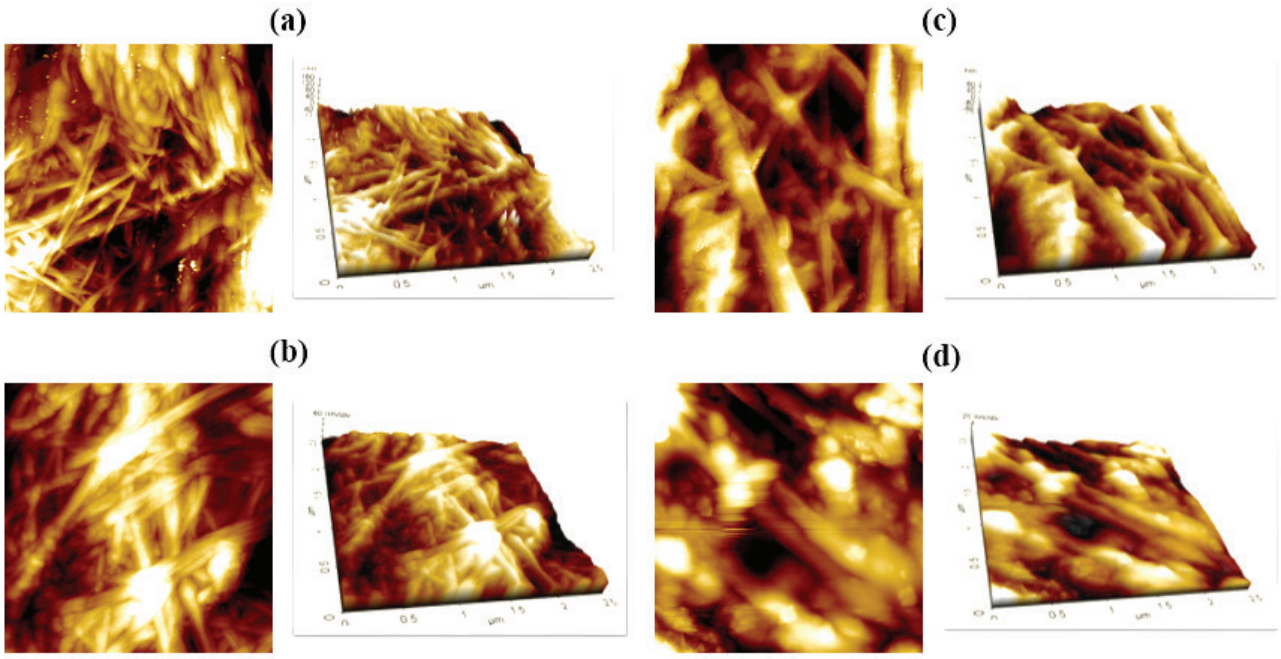

Figure 2. AFM images of all membranes: (a) BC/M0, (b) BC/M1, (c) BC/M2, (d) BC/M3.

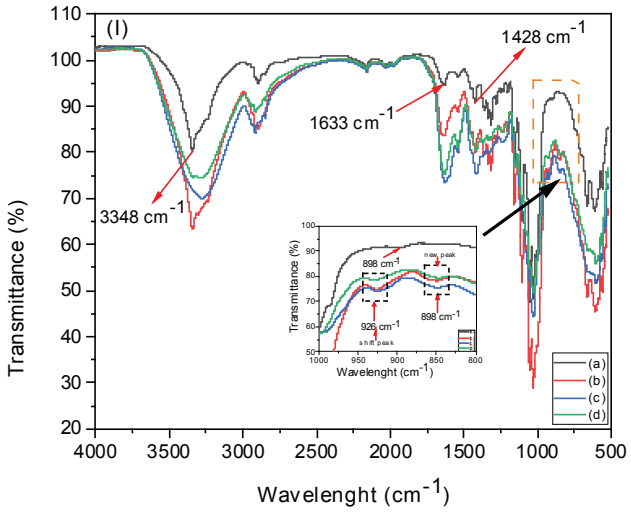

Figure 3. FTIR analysis of (I) All samples: (a) BC/M0, (b-d) BC/M1, BC/M2, BC/M3 composite BC membranes, respectively.

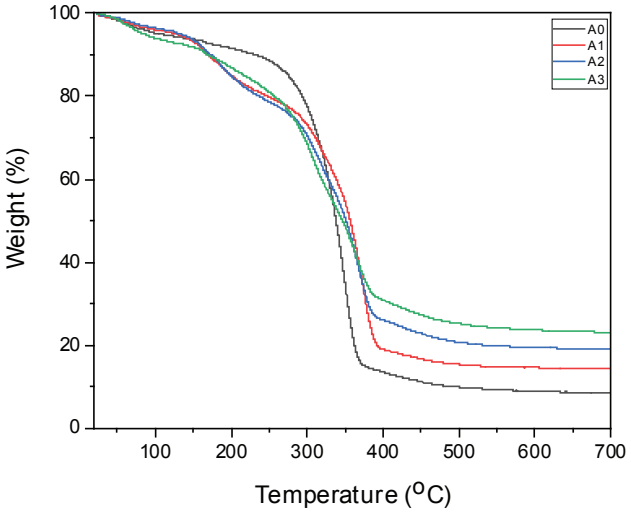

Figure 4. TGA curves of BC/M0, BC/M1, BC/M2 and BC/M3 membranes indicated by A0, A1, A2 and A3, respectively.

Thermal Analysis

The thermal properties of the samples were investigated by the TGA method. The TGA curves of the samples are shown in Figure 4. The samples indicated as A0, A1, A2, and A3 represent BC/M0, BC/M1, BC/M2, and BC/M3, respectively.

As seen in Figure 4. three degradation temperatures for pure BC exist. The first degradation temperature between 10-100 °C is associated with a slight weight loss (about 5%) of the broken inter and intra-molecular hydrogen bonds [46]. The largest mass loss (≈82 wt%), which is associated with depolymerization and pyrolytic decomposition in pure BC, was found to occur between 100-400 °C [47,48]. The mass loss of the BC/*Myrrh* composite after the addition of 5% *myrrh* by mass to pure BC was approximately 68%. This result can be attributed to the fact that the composite structure is more stable due to stronger hydrogen bonding and higher crystallinity. This result is supported by FTIR and XRD data.

X-Ray Diffraction (XRD) Analysis

Cellulose occurs naturally in two polymorphic forms, cellulose I and cellulose II [49]. Cellulose-I has a parallel chain structure and constitutes the natural form of cellulose [50]. The BC we produce also has the cellulose-I structure. The XRD patterns of all the samples were recorded, and the results are illustrated in Figure 5. As shown in Figure 5. centered at 2θ=14.56°, 17.07°, 19.68°, 22.74° and 25.52° indexed as (100), (010), (002), (110) and (114) [51,52] was observed in the XRD pattern of (pure BC), which is attributed to respectively in the triclinic unit cell of allomorph Iα [53], which are usually attributed to crystallographic planes of 100 (amorphous region), 010 (amorphous region), and 110 (crystalline region), respectively [54,55]. In addition, it can be seen from the X-ray diffraction image that the crystallization peak (110) is higher as a result of less amorphization during the production of pure BC. This result is an indication of hydrogen bond formation which is also supported by the FTIR result [34]. The relative crystal index (%CrI) and crystal lattice spacing (d-spacing) obtained from XRD patterns are critical factors affecting the properties of cellulose. The relative crystal index (% CrI) of all samples was found using peak height methods and the results are given in Table 1. The following equation was used for the Segal method [56].

$$\% \, CrI = \frac{I_{110} - I_{am.}}{I_{110}} \, x \, 100 \qquad (2)$$

Where I_{110} and $I_{am.}$ are the maximum intensities of both crystalline and amorphous regions, respectively. It can be seen from Table 1 when 5% *myrrh* was added to BC, the incorporation of *myrrh* into bacterial cellulose increased the crystal index of BC by 13%. This phenomenon can be explained by the increase in intramolecular and intermolecular hydrogen bonds formed as a result of the interaction of OH groups in the *myrrh* molecule with hydroxyl groups in the cellulose structure [57,58]. When these results are evaluated, it can be concluded that there are strong interactions between *myrrh* molecules and the cellulose structure.

The Swelling Analysis of BC and BC/*Myrrh* Membranes

The water holding capacity of Pure BC and BC/*Myrrh* composite membranes was determined by swelling test (Fig. 6). The hydrophilic nature of BC enables it to hold a high amount of water [59]. The water holding capacity of BC is related to its porous structure and surface area. The addition of secondary structures to cellulose influences its physicomechanical properties, thus resulting in differences

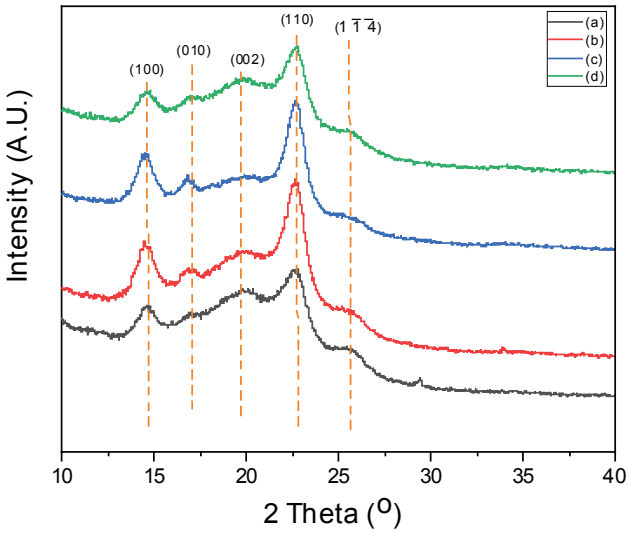

Figure 5. XRD pattern of (a) BC/M0, (b-d) BC/M1, BC/M2, BC/M3 composite BC membranes, respectively.

in the water holding capacity [60]. The swelling rates of the membranes in the first 30 min were about 5 times for pure BC and about 3 times for all BC/*Myrrh* membranes, relative to their dry weights. The swelling rate continued with a significant increase for pure BC and a slower increase for *myrrh* doped membranes. Pure BC had a higher water retention capacity. This is due to the presence of *myrrh* extract molecules penetrating the pure BC between the BC fibers [61]. After 24 h, the water holding capacity of BC/M0, BC/M1, BC/M2, and BC/M3 membranes were 1090.5%, 595.8%, 267.3%, and 137.8%, respectively. The t-test analysis reveals statistically significant differences in swelling behavior between the control membrane (BC/M0) and the *myrrh*-doped membranes (BC/M1, BC/M2, BC/M3) across the tested time intervals ($p < 0.05$). The water holding capacity of BC varies with the integration of substances such as drugs, nanoparticles, polymers, chemical agents, and plant extracts into the structure [62-64]. In the study, composite BC membranes retained a lower amount of water due to the closure of the existing pores of *myrrh*-doped BC. Accordingly, it can be concluded that the swelling test results are directly proportional to the SEM analysis. Providing a moist environment is one of the most critical issue for stimulated wound healing [22]. In this study, we evaluated that *myrrh-doped* cellulose membranes are wound dressings with sufficient swelling ratio because although swelling rates decrease with *myrrh* addition, the swelling analysis results are compatible with the other wound dressing materials reported in the literature [65].

Table 1. Relative crystal index (%CrI) and d-spacing (nm) due to *myrrh* effect on bacterial cellulose from XRD patterns: BC/M0, BC/M1, BC/M2, and BC/M3

Samples	BC/M0	BC/M1	BC/M2	BC/M3
% CrI	61.32	49.81	53.51	69.41
I_{110}	1238.97	1600.58	1172.71	1041.26
I_{100}	479.15	803.22	545.16	318.48

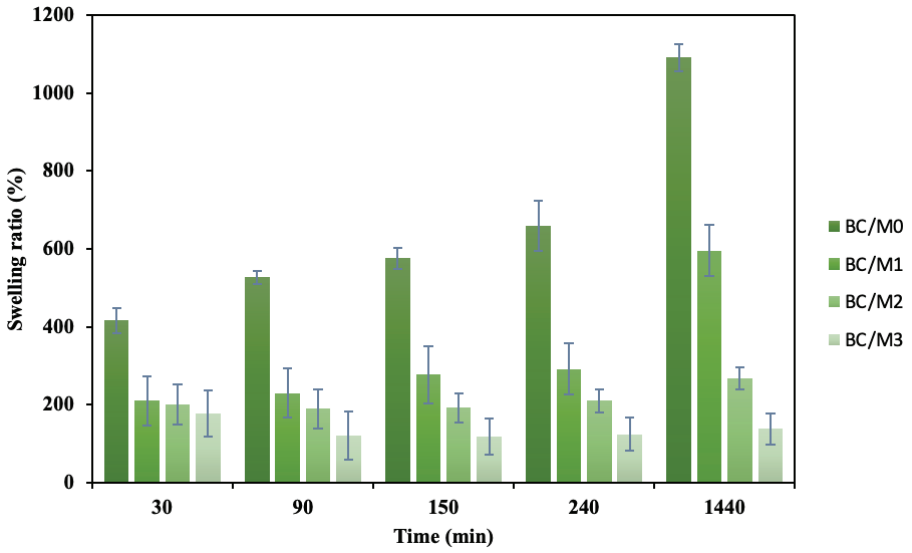

Figure 6. Water holding capacities of pure BC and BC/*Myrrh* membranes.

Cell Viability

The cytotoxicity assay of the membranes was determined by MTT assay on the L929 fibroblast cell line. The cytotoxic effects of *myrrh*-modified BC membranes on cell viability were assessed through t-test analysis at a significance level of $p<0.05$, as presented in Figure 7. The negative control in the graph represents living cells, while the positive control represents dead cells. Cell viability in pure BC membranes was measured as 85.87% (standard error ±3.17). In BC membranes with mixtures of myrrh, cell viability was found to be 88.92% (±2.32), 92.98% (±2.64), and 82.31% (±1.52), respectively. According to the MTT analysis, cell viability was over 80% in pure BC and all membranes containing different ratios of myrrh, and no significantly cytotoxicity was observed. In addition, the BC membrane containing 2.5% myrrh showed the highest cell viability at 92.98% (±2.64). This ratio indicates that the cells survived better without toxicity. The results are similar to previous studies in the literature [66]. Ajiteru et al. reported that *myrrh*-containing hydrocolloid wound dressing developed for wound healing stimulated cell proliferation in the CCK-8 cell line [67]. The fact that BC membranes are biocompatible [68] and positively support cell viability has been supported by studies on different cell lines such as glioblastoma [69], endothelium [70], fibroblast [61], and epithelium [71] with BC modified with different components.

Cell Adhesion

Fibroblast cell presence and proliferation are essential in wound healing since these cells migrate into the wound area and synthesize various collagen types that contribute to tissue repair [72]. For this reason, the L929 cell line was selected, and the adhesion and proliferation rates on the membranes were monitored on days 1, 3, and 7. The retention capacity of the cells is presented in Figure 8. In the graph, the negative control represents viable cells, while the positive control shows non-viable cells. After 24 hours, the adhesion rate on the pure BC membrane was 98.63% (±2.00). BC membranes containing 1.5%, 2.5%, and 5% myrrh showed adhesion rates of 107.65% (±2.38), 105.44% (±1.75), and 88.94% (±1.16), respectively. On day 3, adhesion on pure BC increased to 121.73% (±4.05), while BC/M1, BC/M2, and BC/M3 recorded 135.86% (± 3.76), 143.65% (± 2.92), and 118.84% (± 3.69). By day 7, adhesion on pure BC was 117.39% (±3.80), and the BC/M1, BC/M2, and BC/M3 composites showed 139.61% (±4.90), 146.92% (±3.18), and 124.56% (±2.48), respectively. Pure BC is known to provide an ECM-like environment that supports cell attachment and proliferation through its structural features [73]. Myrrh-added BC composites were also found to increase cell adhesion and proliferation.

According to the cell adhesion and proliferation analysis results, biofilms containing 2.5% mür were shown to provide higher levels of cell adhesion and proliferation compared to BC without mür and BC with 1.5% and 5% mür added. On the third day, the film structure containing 2.5% murex was the membrane with the highest cell adhesion rate at 143.65% (±2.92). This trend continued similarly on the seventh day, with the cell adhesion rate measured at 146.92% (±3.18). The increase in cell number on the third day was higher in membranes with added *myrrh,* while it was slightly lower in pure BC membranes. On the seventh day, the rate of increase in cell proliferation slowed down due to the increase in *myrrh* concentration. These results show that the addition of 2.5% *myrrh* significantly increases cell adhesion and promotes cell proliferation. This suggests that fibroblast activity, which is

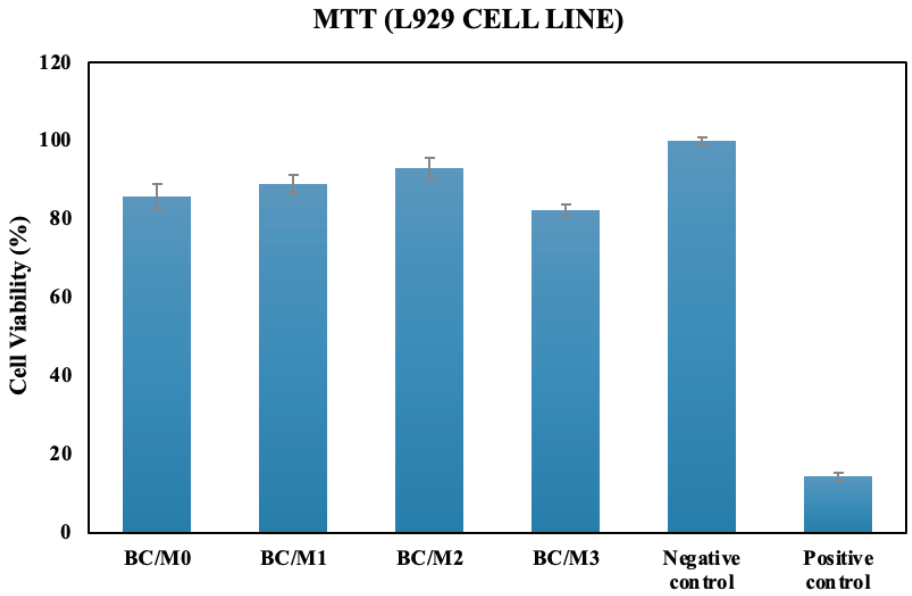

Figure 7. Cytotoxicity results of pure BC and composite BC/*Myrrh* membranes.

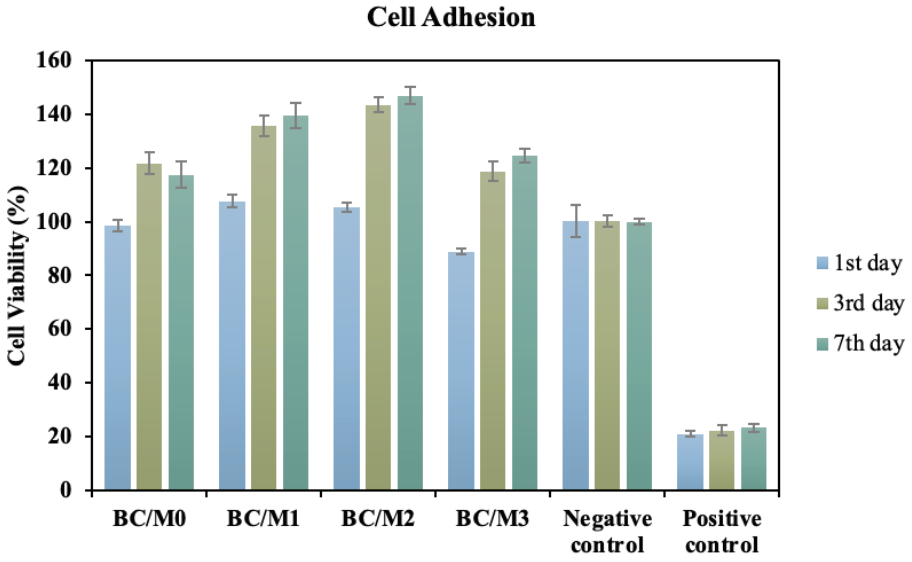

Figure 8. The L929 cell adhesion on membranes.

critical for wound healing, is better supported in this membrane. On the other hand, the lower cell proliferation in the membrane containing 5% *myrrh* may be due to restricted cell adhesion caused by the membrane having a softer surface and smaller pores. The data obtained show that cell adhesion in membranes with added *myrrh* is not statistically significant compared to the negative control ($p>0.05$) but is significantly higher than the positive control ($p<0.001$). Pure BC was found to support cell adhesion and proliferation, and these findings are consistent with previous studies in the literature [66, 74]. In the literature, among the BC hydrogels modified with 10%, 20%, and 30% dextran, materials containing 10% and 20% dextran were reported to have a better proliferation effect on NIH/3T3 mouse fibroblast cells [75]. Previous studies have reported that composite membranes developed by impregnating BC with different components such as aloe vera extract [76,77] alginate [78] and silk sericin [79] have no cytotoxic effect on different cell lines cultured and support cell proliferation. We can say that the results are similar to the literature.

CONCLUSION

This study demonstrated that *myrrh*-doped bacterial cellulose membranes hold strong potential as wound dressing materials by improving fibroblast adhesion, proliferation, and overall biocompatibility. Integrating *myrrh* recognized for its antimicrobial and anti-inflammatory activity into the bacterial cellulose matrix enhanced its biological performance, with the 2.5% *myrrh* formulation showing the most favorable results over the 7-day evaluation period. The in vitro findings indicate that these composite membranes may be effective candidates for advanced wound care, especially in cases where accelerated tissue regeneration is needed. Nevertheless, additional in vivo experiments and clinical studies are required to confirm their therapeutic benefits and to assess long-term behavior, including stability, degradation profile, and antimicrobial activity under physiological conditions. This study emphasize that combining biopolymers such as bacterial cellulose with natural bioactive compounds like m*yrrh* can produce sustainable and highly effective natural wound dressing materials. Future research may focus on integrating different bioactive molecules or complementary polymers to expand the functional properties of BC-based wound care dressings and support their use in regenerative medicine and biomedical fields.

ACKNOWLEDGMENT

We would like to thank Tanju Özer and the organic and herbal producer Yaren Herbalist for providing the *myrrh* extract.

AUTHORSHIP CONTRIBUTIONS

Seda Genç Şimşek: Investigation, Visualization, Writing-Original Draft, Preparation and characterization of BC membranes, Cell culture studies.

Cenk Denktaş: Investigation, Resources, Writing-Original Draft, Preparation and characterization of *Myrrh* doped-BC membranes.

Nelisa Türkoğlu: Resources, Writing-Original Draft, Cell culture studies.

DATA AVAILABILITY STATEMENT

The authors confirm that the data that supports the findings of this study are available within the article. Raw data that support the finding of this study are available from the corresponding author, upon reasonable request.

CONFLICT OF INTEREST

The author declared no potential conflicts of interest with respect to the research, authorship, and/or publication of this article. ETHICS There are no ethical issues with the publication of this manuscript.

STATEMENT ON THE USE OF ARTIFICIAL INTELLIGENCE

Artificial intelligence was not used in the preparation of the article.

REFERENCES

[1] Ijaola AO, Akamo DO, Damiri F, Akisin CJ, Bamidele EA, Ajiboye EG, Berrada M, Onyenokwe VO, Yang SY, Asmatulu E. Polymeric biomaterials for wound healing applications: a comprehensive review. J Biomater Sci Polym Ed 2022;33:1998–2050. [CrossRef]

[2] Takeo M, Lee W, Ito M. Wound healing and skin regeneration. Cold Spring Harb Perspect Med 2015;5:1. [CrossRef]

[3] Sorg H, Tilkorn DJ, Hager S, Hauser J, Mirastschijski U. Skin wound healing: An update on the current knowledge and concepts. Eur Surg Res 2017;58:81–94. [CrossRef]

[4] Tottoli EM, Dorati R, Genta I, Chiesa E, Pisani S, Conti B. Skin wound healing process and new emerging technologies for skin wound care and regeneration. Pharmaceutics 2020;12:80735. [CrossRef]

[5] Morton LM, Phillips TJ. Wound healing and treating wounds: Differential diagnosis and evaluation of chronic wounds. J Am Acad Dermatol 2016;74:589–605; quiz 605–6. [CrossRef]

[6] Yalman V, Laçin NT. Development of humic acid and alginate-based wound dressing and evaluation on inflammation. Mater Technol 2019;34:705–717. [CrossRef]

[7] Laçin NT, Demirbilek M, Yalman V. Tissue engineering and wound healing biomaterials. In book: Frontiers in Stem Cell and Regenerative Medicine Research. 8th ed. Saif Zone, Sharjah, U.A.E: Bentham Science Publisher; 2018. [CrossRef]

[8] Mir M, Ali MN, Barakullah A, Gulzar A, Arshad M, Fatima S, Asad M. Synthetic polymeric biomaterials for wound healing: a review. Prog Biomater 2018;7:1–21. [CrossRef]

[9] Ovington LG. Advances in wound dressings. Clin Dermatol 2007;25:33–38. [CrossRef]

[10] Velnar T, Bailey T, Smrkolj V. The wound healing process: an overview of the cellular and molecular mechanisms. J Int Med Res 2009;37:1528–1542. [CrossRef]

[11] Enoch S, Leaper JD. Basic science of wound healing. Reconstructive 2007;117:12S–34S. [CrossRef]

[12] Kaya S, Derman S. Production, characterization and antioxidant activity evaluation of quercetin loaded PLGA nanofibers. Sigma J Eng Nat Sci 2021;9:443–440.

[13] Das S, Baker AB. Biomaterials and nanotherapeutics for enhancing skin wound healing. Front Bioeng 2016;4:82. [CrossRef]

[14] Moon RJ, Martini A, Nairn J, Simonsen J, Youngblood J. Cellulose nanomaterials review: Structure, properties and nanocomposites. Chem Soc Rev 2011;40:3941–3994. [CrossRef]

[15] Ahmed J, Gultekinoglu M, Edirisinghe M. Bacterial cellulose micro-nano fibers for wound healing applications. Biotechnol Adv 2020;38:107549. [CrossRef]

[16] Chawla PR, Bajaj IB, Survase SA, Singhal RS. Microbial cellulose: Fermentative production and applications. Food Technol Biotechnol 2009;47:107–124.

[17] Mohamad N, Mohd Amin MCI, Pandey M, Ahmad N, Rajab NF. Bacterial cellulose/acrylic acid hydrogel synthesized via electron beam irradiation: Accelerated burn wound healing in an animal model. Carbohydr Polym 2014;114:312–320. [CrossRef]

[18] Khalid A, Madni A, Raza B, Islam MU, Hassan A, Ahmad F, et al. Multiwalled carbon nanotubes functionalized bacterial cellulose as an efficient healing material for diabetic wounds. Int J Biol Macromol 2022;203:256–267. [CrossRef]

[19] Foong CY, Hamzah MSA, Razak SIA, Saidin S, Nayan NHM. Influence of poly (lactic acid) layer on the physical and antibacterial properties of dry bacterial cellulose sheet for potential acute wound healing materials. Fibers Polym 2018;19:263–271. [CrossRef]

[20] Wang F, Sun M, Li D, Qin X, Liao Y, Liu X, et al. Multifunctional asymmetric bacterial cellulose membrane with enhanced anti-bacterial and anti-inflammatory activities for promoting infected wound healing. Small 2023;19:202303591. [CrossRef]

[21] Ul-Islam M, Khan S, Ullah MW, Park JK. Bacterial cellulose composites: Synthetic strategies and multiple applications in bio-medical and electro-conductive fields. Biotechnol J 2015;10:1847–1861. [CrossRef]

[22] Sulaeva I, Henniges U, Rosenau T, Potthast A. Bacterial cellulose as a material for wound treatment: Properties and modifications: A review. Biotechnol Adv 2015;33:1247–1261. [CrossRef]

[23] Cesur NP, Zad Ghaffari Vahdat K, Türkoğlu Laçin N. Fabrication of bacterial cellulose/PVP nanofiber composites by electrospinning. Biopolymers 2024;62:23606. [CrossRef]

[24] Jipa IM, Stoica-Guzun A, Stroescu M. Controlled release of sorbic acid from bacterial cellulose based mono and multilayer antimicrobial films. LWT 2012;47:400–406. [CrossRef]

[25] Erenler R, Çarlik ÜE, Aydin A. Antiproliferative activity and cytotoxic effect of essential oil and water extract from Origanum vulgare L. Sigma J Eng Nat Sci 2023;41:202–208. [CrossRef]
[26] Qiu Y, Qiu L, Cui J, Wei Q. Bacterial cellulose and bacterial cellulose-vaccarin membranes for wound healing. Mater Sci Eng C 2016;59:303–309. [CrossRef]
[27] Manan S, Ullah MW, Ul-Islam M, Shi Z, Gauthier M, Yang G. Bacterial cellulose: Molecular regulation of biosynthesis, supramolecular assembly, and tailored structural and functional properties. Prog Mater Sci 2022;47:100972. [CrossRef]
[28] Ul-Islam M, Alhajaim W, Fatima A, Yasir S, Kamal T, Abbas Y, et al. Development of low-cost bacterial cellulose-pomegranate peel extract-based antibacterial composite for potential biomedical applications. Int J Biol Macromol 2023 Mar 15;231:123269. [CrossRef]
[29] Zhijiang C, Guang Y. Bacterial cellulose/collagen composite: Characterization and first evaluation of cytocompatibility. J Appl Polym Sci 2011;120:2938–2944. [CrossRef]
[30] Fatima A, Yasir S, Khan MS, Manan S, Ullah MW, Ul-Islam M. Plant extract-loaded bacterial cellulose composite membrane for potential biomedical applications. J Bioresour Bioproducts 2021;6:26–32. [CrossRef]
[31] Zmejkoski D, Spasojević D, Orlovska I, Kozyrovska N, Soković M, Glamočlija J, et al. Bacterial cellulose-lignin composite hydrogel as a promising agent in chronic wound healing. Int J Biol Macromol 2018;118:494–503. [CrossRef]
[32] Lin WC, Lien CC, Yeh HJ, Yu CM, Hsu SH. Bacterial cellulose and bacterial cellulose-chitosan membranes for wound dressing applications. Carbohydr Polym 2013;94:603–611. [CrossRef]
[33] Tercjak A, Gutierrez J, Barud HS, Domeneguetti RR, Ribeiro SJL. Nano- and macroscale structural and mechanical properties of in situ synthesized bacterial cellulose/PEO-b-PPO-b-PEO biocomposites. ACS Appl Mater Interfaces 2015;7:4142–4150. [CrossRef]
[34] Ciolacu D, Ciolacu F, Popa VI. Amorphous cellulose—structure and characterization. Cellul Chem Technol 2011;45:13–21.
[35] Tian X, Chengcheng G, Yang Y, Shen X, Huang M, Shaowei LiuRetention and release properties of cinnamon essential oil in antimicrobial films based on chitosan and gum arabic. Food Hydrocoll 2018;84:84–92. [CrossRef]
[36] Rani MU, Udayasankar K, Appaiah KAA. Properties of bacterial cellulose produced in grape medium by native isolate Gluconacetobacter sp. J Appl Polym Sci 2011;120:2835–2841. [CrossRef]
[37] Schenzel K, Fischer S, Brendler E. New method for determining the degree of cellulose I crystallinity using FT Raman spectroscopy. Cellulose 2005;12:223–231. [CrossRef]
[38] Atykyan N, Revin V, Shutova V. Raman and FT-IR spectroscopy investigation the cellulose structural differences from bacteria Gluconacetobacter sucrofermentans during the different regimes of cultivation on a molasses media. AMB Express 2020;10:1. [CrossRef]
[39] Mohd Amin MCI, Ahmad N, Halib N, Ahmad I. Synthesis and characterization of thermo- and pH-responsive bacterial cellulose/acrylic acid hydrogels for drug delivery. Carbohydr Polym 2012;88:465–473. [CrossRef]
[40] Barud HS, Souza JL, Santos DB, Crespi MS, Ribeiro CA, Messaddeq Y, et al. Bacterial cellulose/poly(3-hydroxybutyrate) composite membranes. Carbohydr Polym 2011;83:1279–1284. [CrossRef]
[41] Sun D, Yang J, Wang X. Bacterial cellulose/TiO2 hybrid nanofibers prepared by the surface hydrolysis method with molecular precision. Nanoscale 2010;2:287–292. [CrossRef]
[42] Li D, Ao K, Wang Q, Lv P, Wei Q. Preparation of Pd/bacterial cellulose hybrid nanofibers for dopamine detection. Molecules 2016;21:618. [CrossRef]
[43] Wang SS, Han YH, Ye YX, Shi XX, Xiang P, Chen DL, et al. Physicochemical characterization of high-quality bacterial cellulose produced by Komagataeibacter sp. strain W1 and identification of the associated genes in bacterial cellulose production. RSC Adv 2017;7:45145–45155. [CrossRef]
[44] Gigliarelli G, Becerra JX, Curini M, Marcotullio MC, Forti L. Chemical composition and biological activities of fragrant Mexican copal (Bursera spp.). Molecules 2015;20:22383–22394. [CrossRef]
[45] Martín-Ramos P, Fernández-Coppel IA, Ruíz-Potosme NM, Martín-Gil J. Potential of ATR-FTIR spectroscopy for the classification of natural resins. Biol Eng Med Sci Rep 2018;4:3–6. [CrossRef]
[46] George J, Ramana KV, Sabapathy SN, Jagannath JH, Bawa AS. Characterization of chemically treated bacterial (Acetobacter xylinum) biopolymer: Some thermo-mechanical properties. Int J Biol Macromol 2005;37:189–194. [CrossRef]
[47] Surma-Ślusarska B, Presler S, Danielewicz D. Characteristics of bacterial cellulose obtained from Acetobacter xylinum culture for application in papermaking. Fibres Text East Eur 2008;16:108–111.
[48] Kumar V, Sharma DK, Sandhu PP, Jadaun JJ, Sangwan RS, Yadav SK. Sustainable process for the production of cellulose by an Acetobacter pasteurianus RSV-4 (MTCC 25117) on whey medium. Cellulose 2021;28:103–116. [CrossRef]
[49] Paul RA. Occurrence and functions of native cellulose. California, USA: CRC Press; 1991.
[50] Tsekos I. The sites of cellulose synthesis in algae: Diversity and evolution of cellulose-synthesizing enzyme complexes. J Phycol 1999;35:635–655. [CrossRef]

[51] Lopes TD, Riegel-Vidotti IC, Grein A, Tischer CA, Faria-Tischer PCS. Bacterial cellulose and hyaluronic acid hybrid membranes: Production and characterization. Int J Biol Macromol 2014;67:401–408. [CrossRef]
[52] Hult EL, Iversen T, Sugiyama J. Characterization of the supermolecular structure of cellulose in wood pulp fibres. Cellulose 2003;10:103–110. [CrossRef]
[53] Sugiyama J, Persson J, Chanzy H. Combined infrared and electron diffraction study of the polymorphism of native celluloses. Macromolecules 1991;24:2461–2466. [CrossRef]
[54] Wada M, Sugiyama J, Okano T. Native celluloses on the basis of two crystalline phase (Iα/Iβ) system. J Appl Polym Sci 1993;49:1491–1496. [CrossRef]
[55] Lee CM, Gu J, Kafle K, Catchmark J, Kim SH. Cellulose produced by Gluconacetobacter xylinus strains ATCC 53524 and ATCC 23768: Pellicle formation, post-synthesis aggregation and fiber density. Carbohydr Polym 2015;133:270–276. [CrossRef]
[56] Segal L, Creely JJ, Martin AE, Conrad CM. An empirical method for estimating the degree of crystallinity of native cellulose using the X-ray diffractometer. Textile Res J 1952;29:786–794. [CrossRef]
[57] Singh R, Mathur A, Goswami N, Mathur G. Effect of carbon sources on physicochemical properties of bacterial cellulose produced from Gluconacetobacter xylinus MTCC 7795. E-Polymers 2016;16:331–336. [CrossRef]
[58] Pogorelova N, Rogachev E, Digel I, Chernigova S, Nardin D. Bacterial cellulose nanocomposites: Morphology and mechanical properties. Materials (Basel) 2020;13:2249. [CrossRef]
[59] Gorgieva S, Trček J. Bacterial cellulose: Production, modification and perspectives in biomedical applications. Nanomaterials (Basel) 2019 Sep 20;9:1352. [CrossRef]
[60] Shezad O, Khan S, Khan T, Park JK. Physicochemical and mechanical characterization of bacterial cellulose produced with an excellent productivity in static conditions using a simple fed-batch cultivation strategy. Carbohydr Polym 2010;82:173–180. [CrossRef]
[61] Wang J, Wan YZ, Luo HL, Gao C, Huang Y. Immobilization of gelatin on bacterial cellulose nanofibers surface via crosslinking technique. Mater Sci Eng C 2012;32:536–541. [CrossRef]
[62] Lee KY, Quero F, Blaker JJ, Hill CAS, Eichhorn SJ, Bismarck A. Surface only modification of bacterial cellulose nanofibres with organic acids. Cellulose 2011;18:595–605. [CrossRef]
[63] Ybañez MG, Camacho DH. Designing hydrophobic bacterial cellulose film composites assisted by sound waves. RSC Adv 2021;11:32873–32883. [CrossRef]
[64] Kamal T, Ul-Islam M, Khan SB, Bakhsh EM, Chani MTS. Development of plant extract impregnated bacterial cellulose as a green antimicrobial composite for potential biomedical applications. Ind Crops Prod 2022;187:115337. [CrossRef]
[65] Ul-Islam M, Khan T, Park JK. Water holding and release properties of bacterial cellulose obtained by in situ and ex situ modification. Carbohydr Polym 2012;88:596–603. [CrossRef]
[66] Sanchavanakit N, Sangrungraungroj W, Kaomongkolgit R, Banaprasert T, Pavasant P, Phisalaphong M. Growth of human keratinocytes and fibroblasts on bacterial cellulose film. Biotechnol Prog 2006;22:1194–1199. [CrossRef]
[67] Ajiteru O, Lee OJ, Kim JH, Lee YJ, Lee JS, Lee H, et al. Fabrication and characterization of a myrrh hydrocolloid dressing for dermal wound healing. Colloids Interface Sci Commun 2022;48:100617. [CrossRef]
[68] Pértile RA, Moreira S, Gil da Costa RM, Correia A, Guãrdao L, Gartner F, et al. Bacterial cellulose: Long-term biocompatibility studies. J Biomater Sci Polym Ed 2012;23:1339–1354. [CrossRef]
[69] Unal S, Arslan S, Yilmaz BK, Oktar FN, Sengil AZ, Gunduz O. Production and characterization of bacterial cellulose scaffold and its modification with hyaluronic acid and gelatin for glioblastoma cell culture. Cellulose 2021;28:117–132. [CrossRef]
[70] Cesur NP, Laçin NT. Construction of vascular graft by 3D printing using bacterial cellulose formulation as bioink. Cellulose Chem Technol 2022;56:99–113. [CrossRef]
[71] Shao W, Wu J, Liu H, Ye S, Jiang L, Liu X. Novel bioactive surface functionalization of bacterial cellulose membrane. Carbohydr Polym 2017;178:270–276. [CrossRef]
[72] Ross R, Everett NB, Tyler R. Wound healing and collagen formation VI. The origin of the wound fibroblast studied in parabiosis. J Cell Biol 1970;44:645–654. [CrossRef]
[73] Halib N, Ahmad I, Grassi M, Grassi G. The remarkable three-dimensional network structure of bacterial cellulose for tissue engineering applications. Int J Pharm 2019;566:631–640. [CrossRef]
[74] Andrade FK, Alexandre N, Amorim I, Gartner F, Mauricio AC, Luis AL, et al. Studies on the biocompatibility of bacterial cellulose. J Bioact Compat Polym 2013;28:97–112. [CrossRef]
[75] Lin SP, Kung HN, Tsai YS, Tseng TN, Di Hsu K, Cheng KC. Novel dextran modified bacterial cellulose hydrogel accelerating cutaneous wound healing. Cellulose 2017;24:4927–4937. [CrossRef]
[76] Godinho JF, Berti FV, Müller D, Rambo CR, Porto LM. Incorporation of Aloe vera extracts into nanocellulose during biosynthesis. Cellulose 2016;23:545–555. [CrossRef]

[77] Ul-Islam M, Ahmad F, Fatima A, Shah N, Yasir S, Ahmad MW, et al. Ex situ synthesis and characterization of high strength multipurpose bacterial cellulose-Aloe vera hydrogels. Front Bioeng Biotechnol 2021;9:601988. [CrossRef]

[78] Chiaoprakobkij N, Sanchavanakit N, Subbalekha K, Pavasant P, Phisalaphong M. Characterization and biocompatibility of bacterial cellulose/alginate composite sponges with human keratinocytes and gingival fibroblasts. Carbohydr Polym 2011;85:548–553. [CrossRef]

[79] Lamboni L, Li Y, Liu J, Yang G. Silk sericin-functionalized bacterial cellulose as a potential wound-healing biomaterial. Biomacromolecules 2016;17:3076–3084. [CrossRef]